

of surface electrode recordings in patients with symptoms suggestive of polyneuropathy. First, it is important to note that approximately one third of the patients with normal surface electrode recordings had an abnormal near-nerve result. This is probably due to a better-defined normative reference range for the near-nerve recordings compared to the surface electrode recordings, which can be explained by the fact that the amplitude of the sensory nerve action potential is much larger when the near-nerve technique is applied (Fig. 2, example 1) and that abnormal configuration of the potential is predominantly found with the near-nerve recordings. This result is comparable with previous studies (Rajabally et al., 2009), and underlines the relatively low sensitivity of the sural nerve surface electrode recordings. Second, in approximately two thirds of the patients, for whom no response was seen using surface electrodes, an abnormal response was found using the near-nerve technique (Fig. 2, example 2). None of these patients, however, had a normal near-nerve examination, which is reassuring. Obtaining an abnormal result rather than no response can be important in relation to the classification of the polyneuropathy as axonal or demyelinating, but most of the demyelinating polyneuropathy patients had demyelinating features in several nerves. The largest increase in sensitivity was seen in patients with an axonal polyneuropathy. Recently, a new technique for sural nerve conduction studies using on-nerve needle recordings during sural nerve biopsy has been described and compared to surface electrode recordings and histopathological findings in 89 polyneuropathy patients (Oh et al., 2015). These recordings had a better concordance with nerve biopsy findings than surface electrode recordings and in 15% of the patients a sensory nerve action potential was obtained using the on-nerve recordings although surface electrode recordings showed no response. Interestingly, the same was true in 13% of our polyneuropathy patients. Although the patient populations are not fully comparable these results suggest that near-nerve and on-nerve recordings increase sensitivity by approximately the same magnitude. In clinical practice, an important limitation to the near-nerve technique is that it can be quite time consuming, and that some patients find it painful. Furthermore, execution of the procedure does require some experience. Special attention must be given to the distance between stimulation and recording electrodes as the amplitude of the potential decreases with increasing distance (Horowitz and Krarup, 1992) and to the placement of the stimulating electrode using the predefined stimulation threshold.

In conclusion, the results of our study suggest that sural nerve surface recordings should be accompanied by other measures of sensory nerve conduction in the lower extremity such as near-nerve recordings or surface electrode recordings of the distal sensory nerves if normal values are found in patients with a strong clinical suspicion of polyneuropathy. Future comparative studies of the sensitivity of near-nerve, on-nerve, and distal surface electrode recordings in large samples of polyneuropathy patients could clarify the optimal diagnostic strategy.

Conflict of interest

None of the authors have potential conflicts of interest to be disclosed.

References

- Buchthal F, Rosenfalck A. Evoked action potentials and conduction velocity in human sensory nerves. *Brain Res* 1966;3:2–122.
- England JD, Gronseth GS, Franklin G, Miller RG, Asbury AK, Carter GT, et al. Distal symmetric polyneuropathy: a definition for clinical research: report of the American Academy of Neurology, the American Association of Electrodiagnostic Medicine, and the American Academy of Physical Medicine and Rehabilitation. *Neurology* 2005;64:199–207.

- Horowitz SH, Krarup C. Conduction studies of the normal sural nerve. *Muscle Nerve* 1992;15:374–83.
- Oh SJ, Hemmi S, Hatanaka Y. On-nerve needle nerve conduction study in the sural nerve: A new technique for evaluation of peripheral neuropathy. *Clin Neurophysiol* 2015;126:11811–6. <http://dx.doi.org/10.1016/j.clinph.2014.12.008>.
- Rajabally YA, Beri S, Bankart J. Electrophysiological markers of large fibre sensory neuropathy: a study of sensory and motor conduction parameters. *Eur J Neurol* 2009;16:1053–9.
- Singleton JR, Bixby B, Russell JW, Feldman EL, Peltier A, Goldstein J, et al. The Utah Early Neuropathy Scale: a sensitive clinical scale for early sensory predominant neuropathy. *J Peripher Nerv Syst* 2008;13:218–27.
- Uluc K, Isak B, Borucu D, Temucin CM, Cetinkaya Y, Koytak PK, et al. Medial plantar and dorsal sural nerve conduction studies increase the sensitivity in the detection of neuropathy in diabetic patients. *Clin Neurophysiol* 2008;119:880–5.

Thomas Krøigaard *

Department of Neurology, Institute of Clinical Research, University of Southern Denmark, Sdr. Boulevard 29, 5000 Odense C, Denmark

* Tel.: +45 6541 2471; fax: +45 6541 3389.

E-mail address: tkroigaard@health.sdu.dk

Søren H. Sindrup

Department of Neurology, Institute of Clinical Research, University of Southern Denmark, Denmark

Available online 20 August 2015

1388-2457/© 2015 International Federation of Clinical Neurophysiology. Published by Elsevier Ireland Ltd. All rights reserved.
<http://dx.doi.org/10.1016/j.clinph.2015.07.028>

Temporal patterning of neural synchrony in the basal ganglia in Parkinson's disease



Parkinson's disease (PD) is associated with elevated beta-band synchrony and oscillations in cortical and subcortical circuits including subthalamic nucleus (STN) and internal pallidum (GPi) (Hammond et al., 2007). The origin and nature of parkinsonian beta-band synchrony are poorly understood. We previously described temporal patterning of beta-band synchrony in STN (Park et al., 2010). Here, we explore and compare neural synchronization in GPi vs. STN. These nuclei attract special attention, being targets for surgical intervention. Moreover, STN may have a special role in the generation and expression of pathological synchrony because of its mutual excitatory–inhibitory connections with external pallidum. Although STN and GPi differ in function (excitatory vs. inhibitory), anatomical architecture, and connectivity, they both exhibit parkinsonian beta-band synchrony. Comparative analysis of synchrony properties may help in understanding the involvement of both nuclei in pathological parkinsonian neural activity.

This study includes eight PD patients undergoing microelectrode-guided DBS electrodes implantation. The study was approved by Indiana University IRB; patients provided informed consent. Four patients had GPi DBS (all male, age 56 ± 7 years, disease duration 11 ± 3 years, UPDRS scores OFF-medication 45 ± 6). These include all GPi DBS patients with available appropriate data. Four other patients had STN DBS (one female, age 69 ± 6 years, disease duration 7 ± 3 years, UPDRS scores OFF-medication 53 ± 9). Electrophysiological recordings were performed with Guideline 4000 (FHC), modified to record spiking units and LFP. The average duration of recorded episodes was 225 ± 45 s. The procedures were described earlier (Park et al., 2010).

The time-series analysis followed (Park et al., 2010). After extracting single units, spiking and LFP signals were band-pass

filtered to the beta-band (defined here as 10–30 Hz). To detect oscillatory episodes, a signal-to-noise ratio criterion (Park et al., 2010) was used. The phases were reconstructed using Hilbert transform (Hurtado et al., 2004). Fig. 1(A) and (B) shows examples of the data. Fig. 1(C) shows the sines of the phases $\phi_{spikes}(t)$ and $\phi_{LFP}(t)$. The spiking/LFP synchrony strength was computed using a phase-locking index:

$$\gamma = \left\| \frac{1}{N} \sum_{j=1}^N e^{i\phi_j} \right\|^2,$$

where $\phi_j = \phi_{spikes}(t_j) - \phi_{LFP}(t_j)$. We considered this index for spiking/LFP synchronization for both GPi and STN. The average (for the sample of all recordings in all patients) value of the synchrony index for STN was found to be 0.16 while for GPi, it was 0.14. An ANOVA test indicated no significant difference between LFP–spike synchronization strength in STN and GPi.

Temporal patterning of synchronization was characterized by the distribution of desynchronization durations (Park et al., 2010; Ahn et al., 2011). Briefly, whenever the phase of one signal

(spiking unit) crosses an arbitrary threshold the value of the phase of the other signal (LFP) is recorded. We utilized episodes with significant phase-locking ($p < 0.05$), estimated with surrogates (Hurtado et al., 2004; Park et al., 2010). Since some level of phase synchronization is present, there is a preferred value of the phase difference. Dynamics is considered to be desynchronized, when the actual phase difference deviates from the preferred phase difference by more than $\pi/2$ as in Park et al. (2010) and Ahn et al. (2011). In this approach the duration of the desynchronized episodes is measured in cycles of the oscillations. This approach distinguishes between a large number of short desynchronizations, a small number of long desynchronizations and the spectrum of possibilities in between even if they all yield the same average value of synchronization strength.

Fig. 1(D) presents desynchronization durations distributions. Distributions have mode = 1 and decay sharply. The desynchronizations lasting for one cycle of oscillations (synch/out of synch/synch) outnumber the next duration, two cycles, by more than a factor of two. The large number of desynchronizations may bring overall synchrony to low levels, but this low level is reached via

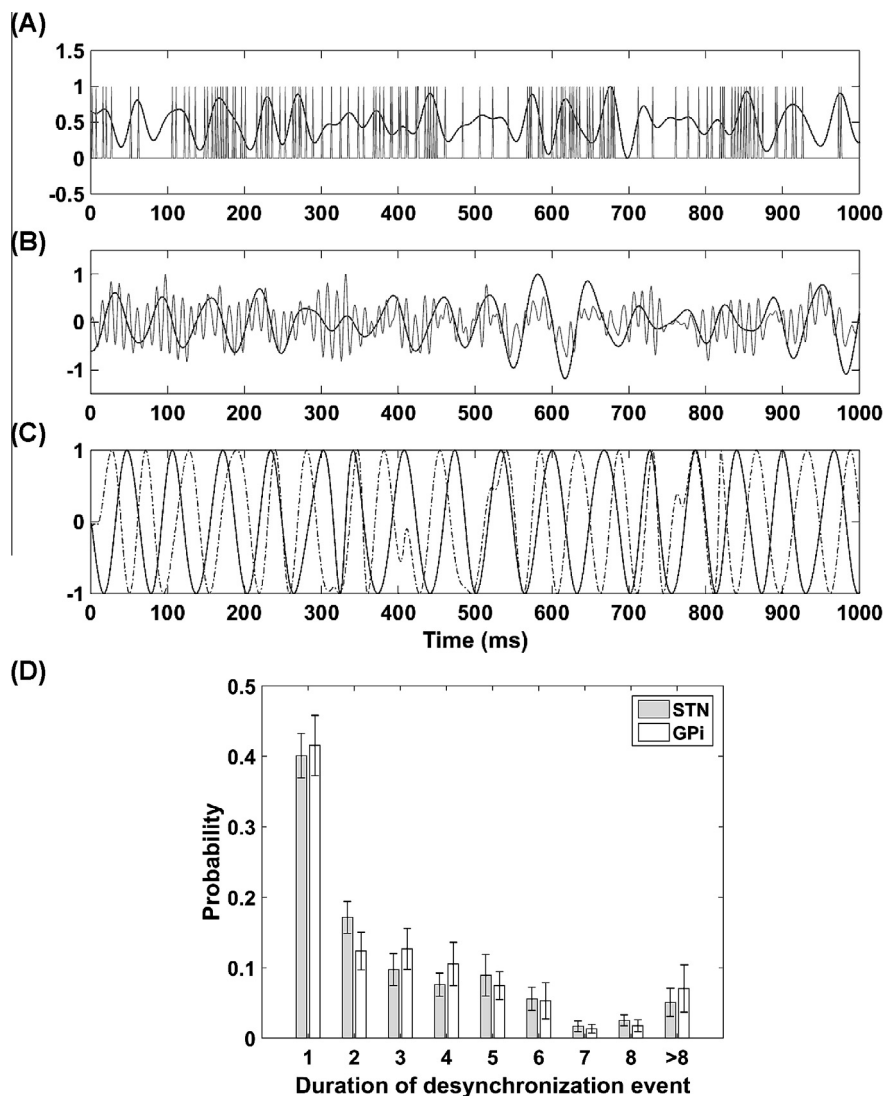


Fig. 1. (A) and (B) Examples of the spiking and filtered spiking signal and raw and filtered LFP signal, respectively. The filtered signals are shown as solid black lines. (C) The sines of the phases of these filtered signals (dotted line – spiking, solid line – LFP). (D) The histogram of probabilities of desynchronization durations (with standard errors) for STN (grey) and GPi (white). Desynchronization durations are measured in cycles of oscillations. For the duration >8, all durations are pooled together so that the last bin accounts for all long durations longer than 8 cycles.

many short desynchronizations (as opposed to a few long desynchronized episodes).

Cycle 1 duration probability is significantly larger than all other probabilities (one-way ANOVA, $p < 10^{-5}$) for both GPi and STN. Thus our analysis indicates that the neural synchronization in GPi as well as in STN is punctuated by numerous episodes of desynchronized activity, most of which are very short-lasting.

In general, a given synchronization strength may be reached with many short or few long desynchronizations, or many possibilities in between (Park et al., 2010; Ahn et al., 2011). However, in the parkinsonian basal ganglia, the moderate synchrony is achieved due to frequent and short interruptions of the synchronized activity, which easily destabilizes and easily reestablishes itself exhibiting intermittent dynamics.

A similar patterning of STN synchrony was reported earlier (Park et al., 2010). So we performed comparative analysis of STN and GPi synchrony. Distributions of desynchronization durations in STN and GPi (Fig. 1(D)) are not significantly different (multivariate ANOVA, $p = 0.8$). Thus the synchrony in GPi and STN exhibits essentially identical temporal patterning. As a check, we performed a similar analysis for alpha and theta frequency bands. Desynchronization duration distributions are statistically different ($p < 0.05$) in between alpha and beta and between theta and beta bands in both STN and GPi activity. In particular, the average desynchronization duration for the beta-band is 1.94 cycles while the average desynchronization duration for alpha and theta bands are lower at 1.43 cycles and 1.29 cycles, respectively. The decay of the distributions (how quickly the chances to observe a desynchronized event decrease with its duration) is frequency-specific too. This indicates that the beta-band dynamics is different from other bands, which fits with the special role of beta in parkinsonism.

Note that the average ages of STN and GPi groups are different and this difference may have an unknown effect on the results. However we suppose that age difference is more likely to increase the difference between STN and GPi, yet our results indicate their similarity. We also note that we have only 4 patients per group, which may negatively affect statistical significance. However, the STN group includes 26 different brain locations, from which good data were recorded, and GPi group has 20 different locations. Furthermore, the total number of desynchronization events is 1660 for STN group and 1335 for GPi group. Hence, the results regarding the properties of desynchronizations are obtained from a small sample of patients but a large sample of desynchronizations.

STN and GPi are very different anatomically: GPi is an inhibitory structure with intranuclear connectivity and inhibitory striatal input, STN is an excitatory structure (likely without intranuclear connectivity). LFPs (believed to be largely formed by synaptic currents) are thus likely to arise in STN and GPi in different ways. Yet, the similarity of temporal patterning of synchrony points to deep similarities in the organization and structure of underlying dynamics (Ahn et al., 2011). Thus the lack of statistically significant differences in the distribution of desynchronization events (and in the average level of synchrony strength) suggests that both STN and GPi belong to a functionally connected group of circuits supporting pathological beta-band synchronized oscillations in PD. Together with the observations of cortico-subcortical interactions (Marreiros et al., 2013) our results support the view that pathological synchronous beta-band oscillations are a non-local phenomena supported by functionally connected internuclear networks of the brain.

Acknowledgements

The study was supported by IU-CRG and the Indiana University Health – Indiana University School of Medicine Strategic Research Initiative.

Conflicts of interest: None of the authors have potential conflicts of interest to be disclosed.

References

- Ahn S, Park C, Rubchinsky LL. Detecting the temporal structure of intermittent phase locking. *Phys Rev E Stat Nonlin Soft Matter Phys* 2011;84:016201.
- Hammond C, Bergmann H, Brown P. Pathological synchronization in Parkinson's disease: networks, models and treatments. *Trends Neurosci* 2007;30:357–64.
- Hurtado JM, Rubchinsky LL, Sigvardt KA. Statistical method for detection of phase-locking episodes in neural oscillations. *J Neurophysiol* 2004;91:1883–98.
- Marreiros AC, Cagnan H, Moran RJ, Friston KJ, Brown P. Basal ganglia–cortical interactions in parkinsonian patients. *Neuroimage* 2013;66:301–10.
- Park C, Worth RM, Rubchinsky LL. Fine temporal structure of beta oscillations synchronization in subthalamic nucleus in Parkinson's disease. *J Neurophysiol* 2010;103:2707–16.
- Shivakeshavan Ratnadurai-Giridharan
Department of Mathematical Sciences and Center for Mathematical Biosciences, Indiana University–Purdue University Indianapolis, Indianapolis, IN, USA
- S. Elizabeth Zaubner
Department of Neurology, Indiana University School of Medicine, Indianapolis, IN, USA
- Robert M. Worth
Department of Mathematical Sciences and Center for Mathematical Biosciences, Indiana University–Purdue University Indianapolis, Indianapolis, IN, USA
- Department of Neurosurgery, Indiana University School of Medicine, Indianapolis, IN, USA
- Thomas Witt
Department of Neurosurgery, Indiana University School of Medicine, Indianapolis, IN, USA
- Sungwoo Ahn
Department of Mathematical Sciences and Center for Mathematical Biosciences, Indiana University–Purdue University Indianapolis, Indianapolis, IN, USA
- Present address: Department of Mathematics, East Carolina University, Greenville, NC, USA
- Leonid L. Rubchinsky*
Department of Mathematical Sciences and Center for Mathematical Biosciences, Indiana University–Purdue University Indianapolis, Indianapolis, IN, USA
- Stark Neurosciences Research Institute, Indiana University School of Medicine, 402 N. Blackford St, Indianapolis, IN 46202, USA
- * Tel.: +1 317 274 9745; fax: +1 317 274 3460.
- E-mail address: leo@math.iupui.edu

Available online 25 September 2015